CD14 modulates age- and injury-induced subchondral bone remodeling in osteoarthritis (OA) via Type I Interferon

Lance A. Murphy[1,2], Kevin G. Burt[1,2], Kate L Sharp[2], Baofeng Hu[1,2], Vu Nguyen[1,2], Robert L. Mauck[1,2], Carla R. Scanzello[1,2]
[1]University of Pennsylvania, Perelman School of Medicine, Philadelphia, PA; [2]CMC VA Medical Center, Translational Musculoskeletal Research Center, Philadelphia, PA. **Disclosures:** LAM (N) - Lance.murphy@pennmedicine.upenn.edu, BH (N), KGB (N), MW (N), VN (N), RLM (5), CRS (8)

INTRODUCTION: While arthritis is generally considered a disease of the joint, its impact on bone is fundamental to disease progression. In erosive arthritis (e.g., rheumatoid arthritis), inflammation impacts endogenous bone cell (osteoblast and osteoclast) activity, resulting in excessive bone resorption (1). Conversely, in osteoarthritis (OA), aberrant bone remodeling results in subchondral sclerosis and osteophyte formation (2). Inflammatory cytokines drive bone erosion and can be targeted in inflammatory arthritis, yet the cellular mechanisms driving aberrant bone formation in OA are not fully established. Our group demonstrated that CD14-deficient mice show less subchondral bone remodeling after joint injury in a destabilization of the medical meniscus (DMM)-model of OA (3). CD14 is a Toll-like Receptor (TLR) activating co-receptor that is highly expressed in myeloid cells, including the precursors of osteoclasts (OCs) (4). Toll-like receptor 4 (TLR4) activation is inhibitory to osteoclastogenesis and can act through multiple pathways, including the sequestration of NF-κB as well as the production of Type I Interferons (IFN-I) (5). Osteoblasts (OBs), on the other hand, are not known to highly express CD14, but TLR4 signaling has been reported to both activate and inhibit their formation (6). To further define the role of CD14 on subchondral bone remodeling, we evaluated subchondral bone formation in CD14-deficient mice in the context of aging- and injury-induced OA models *in vivo*. Further, to understand the signaling that underlies differential OA bone remodeling between CD14-deficient and sufficient strains we assessed OB and OC number *in vivo* and evaluated the capacity for OC differentiation *in vitro*. ***We hypothesized that deficiency or blockade of CD14 would reduce subchondral bone remodeling in murine OA models and protect against TLR4-dependent inhibition of osteoclastogenesis through reduced IFN-I signaling.***

METHODS: Aging Study: WT and CD14-deficient mice were aged to 12 months. Destabilization of the medial meniscus (DMM) (n=14/group): DMM was performed on male C57BL/6 (WT) mice at 12-wks of age. As the DMM model is most consistent in male mice, only male mice were used. For CD14 inhibitor studies, mice were treated intra-articularly with a CD14 inhibitor (.5 mg/kg) or isotype control 3 times within the first 3 weeks post-surgery and sacrificed 12-wks post-surgery. In the CD14KO DMM study, WT and CD14-deficient mice underwent sham and DMM surgeries, and sacrificed 2-wks post-DMM. Micro-CT Imaging: Bone assessments were performed using micro-computed tomography (micro-CT; SkyScan 1174, Bruker). Scanning parameters included an x-ray tube voltage of 50 kV, current of 793 μA, and an exposure time of 1600 ms, with a slice thickness and isotropic voxel size of ~ 9μm. Histology (n=4-5 per group): Mid-joint cryo-sections were stained with ELF97 in acidic buffer to identify Tartrate Resistant Acid Phosphatase (TRAP)-positivity (indicative of OCs), or in basic conditions to identify alkaline phosphatase (ALP) activity (indicative of osteoblasts, OBs). Trabecular surface area covered by OCs or OBs in the medial tibial plateau was measured across five 40X fields per mouse and was normalized by total trabecular surface area (ImageJ). All sections were counterstained with ToPro3 (TP3). Cell isolation and culture: For *in vitro* studies, bone marrow (BM) was pooled from the femorae and tibiae of 3-5 mice from each strain (WT, CD14KO, and Type I interferon receptor (IFNAR1) KO). Cells were cultured in complete αMEM + 30 ng/mL M-CSF for 5 days to expand OC precursors, before exposure to RANKL (100 ng/mL) to induce osteoclastogenesis over 4 days. In some studies, either soluble recombinant CD14 (Abcam, 0.005-0.5 μg/mL) or an anti-IFNAR1 antibody (MAR1-5A3, 1 μg/mL) was added. OC quantification: Cells were stained for TRAP 3 or 4 days after the addition of RANKL and imaged (5 images/well, 4 wells/timepoint), and OCs identified as TRAP+ multinucleated cells. Percent area of the field covered by OCs was reported (CellProfiler). Bulk RNA sequencing: RNA was harvested from WT and CD14-deficient osteoclasts 4 days after the addition of RANKL. Hallmark pathway analysis was used. Statistics: Unpaired t-tests were used to test between groups, with a Holm-Sidak correction for multiple comparisons.

RESULTS: In the aging model, at 12-months of age, the subchondral bone of CD14-deficient mice exhibited decreased bone volume fraction (BVF; bone volume (BV)/total volume (TV)) and trabecular thickness compared to WT mice (**1A**). In the injury-induced DMM model at 12-wks there was increased BVF and bone mineral density (BMD) in the Isotype-treated WT DMM group compared to unoperated mice, which was mitigated by treatment with anti-CD14 antibody (**1B**). At 2-wks following DMM, CD14-deficient mice also demonstrated decreased BVF compared to their WT counterparts. While there was no difference in OB staining area between strains, CD14-deficient mice showed a 3-fold increase in OC area compared to WT (**1C**). *In vitro*, CD14-deficient precursors differentiated into OCs more rapidly than WT cells (**2A**). Treatment of CD14-deficient cells with rCD14 inhibited OC formation in a dose-dependent manner (**2B**). Pathway analysis of bulk RNA sequencing data revealed downregulation of IFN-I signaling in CD14-deficient OCs (**2C**). Notably, OC differentiation of precursors from IFNAR1KO occurred more rapidly than WT cells, phenocopying results from CD14-deficient mice (**2D**). Similarly, treatment of WT cells with an anti-IFNAR1 antibody increased the rate of OC formation, matching that of CD14-deficient cells (**2E**).

DISCUSSION: Using both aging- and injury-induced models of OA, we demonstrated that CD14-deficiency or blockade protects against aberrant bone remodeling. In vivo analysis of subchondral bone demonstrates increased OCs in the absence of CD14, and in vitro functional assays support that this is likely due to aberrant osteoclastogenesis. Mechanistically, CD14-deficient osteoclasts differentiated earlier, and both genetic and pharmacologic approaches indicate that this is due to decreased IFN-I signaling downstream of CD14/TLR activation. Targeting this pathway using an anti-CD14 antibody showed protection against aberrant bone remodeling for up to 12 weeks post-injury in WT mice. These data indicate that CD14 acts to modulate IFN-I signaling to regulate bone remodeling in the setting of joint injury and age. Future studies will validate the role of IFN-I signaling on OA-related bone remodeling *in vivo*. **SIGNIFICANCE/CLINICAL RELEVANCE:** The protection against subchondral bone thickening observed in CD14-deficient mice may be due to the increased presence of OCs. Understanding the role and specific mechanisms of CD14/TLR signaling in osteoclastogenesis may lead to new therapeutic strategies for diseases characterized by pathologic bone remodeling. Additionally, targeting downstream pathways of CD14/TLR signaling, including IFN-I, identify new druggable therapeutic targets that could be used to treat OA and other diseases of aberrant bone remodeling. **REFERENCES:**

[1] Niu+ *Front Immunol* 2022 [2]Donell+ *EFORT* 2019; [3] Sambamurthy+ *PLoS ONE 2018*; [4] Zanoni+ *Front Cell Infect. Microbiol.* 2013; [4] Xue+ *Art Res Ther* 2020; [5] Souza+ *Front Immunol* 2019 [6] Alonso-Perez+ *Sec. Integrative Physiology* 2018

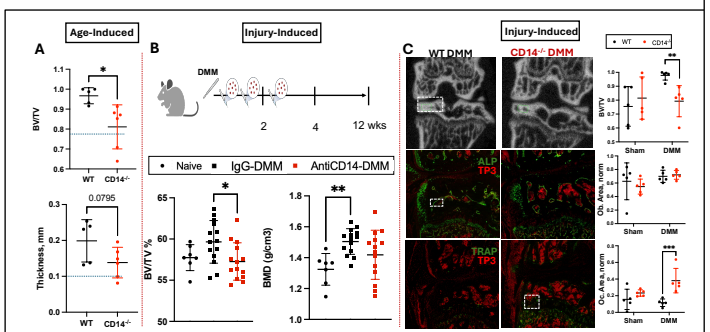

Figure 1: BVF and trabecular thickness of 12 month old (MO) WT and CD14$^{-/-}$ mice; dashed line denotes 4MO control (A). BVF and BMD of WT mice 16 weeks post-DMM following treatment with anti-CD14 antibody or isotype control (B). Images and quantification of BVF (box outlines region of interest), osteoblast area (box outlines area of positive ALP signal), and osteoclast area (box outlines area of positive TRAP signal) in WT and CD14$^{-/-}$ mice 2-wks post-DMM (C). *p<0.05, **p<0.01, ***p<0.005.

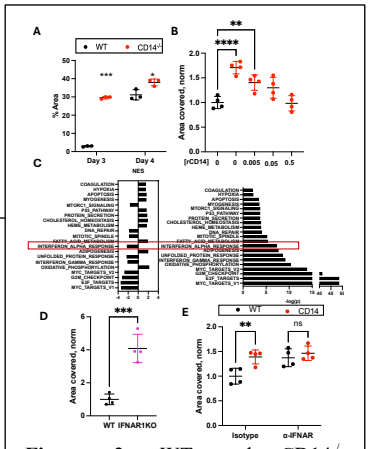

Figure 2: WT and CD14$^{-/-}$ osteoclastogenesis (OC-genesis) on days 3 and 4 post-RANKL addition (A). WT and CD14-deficient OC-genesis with rCD14 treatment for 3 days (B). Pathway analysis of DEGs for WT and CD14$^{-/-}$ OCs (C). OC-genesis of WT and IFNAR1$^{-/-}$ cells on day 3 (D). OC-genesis of WT and CD14$^{-/-}$ cells treated with anti-IFNAR1 antibody for 3 days (E).